

# Enhancing the Prediction Capabilities for Barrette Wall Displacement Using the Finite Element Method and Artificial Neural Networks

**Truong Xuan Dang**

Ho Chi Minh University of Natural Resources and Environment, Ho Chi Minh City, Vietnam  
dxtruong@hcmunre.edu.vn

**Tuan Anh Nguyen**

University of Transport Ho Chi Minh City, Ho Chi Minh City, Vietnam  
tuanna@ut.edu.vn (corresponding author)

**Luan Nhat Vo**

Van Hien University, Ho Chi Minh City, Vietnam  
luanvn@vhu.edu.vn

**Hoa Van Vu Tran**

The SDCT Research Group, University of Transport Ho Chi Minh City, Ho Chi Minh City, Vietnam  
hoa.tranvu.htgroup@gmail.com

Received: 21 April 2025 | Revised: 5 June 2025 | Accepted: 14 June 2025

Licensed under a CC-BY 4.0 license | Copyright (c) by the authors | DOI: <https://doi.org/10.48084/etasr.11631>

## ABSTRACT

This study aimed to evaluate the lateral displacement of barrette walls in underground construction projects using the Finite Element Method (FEM) and an Artificial Neural Network (ANN). Lateral displacement analysis is crucial to ensure the safety and stability of structures, especially under complex geological conditions. FEM is used to simulate the displacement of barrette walls with varying thicknesses (400, 600, 800, and 1000 mm), while the ANN is applied to predict displacement based on FEM data, enhancing accuracy and analysis efficiency. The FEM results were compared with real-world data obtained from an inclinometer for an 800 mm thick barrette wall, showing a high correlation that confirms the model's reliability. The ANN model achieved high  $R^2$  values in predicting displacements, with 0.9998 for the Uy direction and 0.9887 for the Ux direction, demonstrating its ability to accurately replicate lateral displacements. This study confirms that the combination of FEM and ANN can improve displacement prediction capabilities, laying the foundation for optimizing design and ensuring safety in underground structures. By utilizing FEM and ANN, this study not only enhances the accuracy of analyses but also contributes to the development of more effective prediction tools, supporting the design and construction processes of underground infrastructure in complex urban environments.

**Keywords-**finite element method; artificial neural network; horizontal displacement prediction; barrette walls; displacement

## I. INTRODUCTION

Barrette walls are a crucial component in ensuring the stability of underground infrastructure. These structures often face complex geological conditions and the influence of soil and groundwater pressures. Therefore, accurately predicting the lateral displacement of barrette walls is essential to ensure safety and efficiency during the design and construction phases [1-5]. An accurate prediction can help minimize the risks of structural failure and optimize construction costs, contributing to the sustainability and safety of the project. FEM has been

widely used to analyze lateral displacements in structures, such as retaining and barrette walls. FEM allows detailed simulations of structural behavior under complex factors, such as geological forces and environmental conditions, providing reliable and precise results [6]. However, FEM can encounter challenges in fully modeling nonlinear elements, necessitating supplementary methods. In this context, ANNs have emerged as a powerful tool for predicting lateral displacement, thanks to their ability to learn and model non-linear relationships from large datasets [7, 8], thus enhancing the predictive capacity and supporting FEM analysis.

Previous studies have shown that combining FEM with artificial intelligence methods such as ANNs can improve the accuracy of displacement predictions [9, 10]. Some studies have demonstrated that an ANN can learn from FEM data to create faster and more precise predictive models, especially when applied to complex geological conditions [11-14]. These studies also highlight the effectiveness of ANN in complementing and extending traditional analyses, increasing applicability in infrastructure design and construction. Based on this background, this study aimed to evaluate the capacity of FEM to predict the lateral displacement of barrette walls and to validate its accuracy using real observational data. Simultaneously, the study focuses on an ANN to predict displacement based on FEM output data, evaluating the combined use of these two methods in geotechnical analysis. The research question posed is whether ANN can complement and enhance FEM's lateral displacement predictions and to what extent this model aligns with real geological conditions. This study seeks to contribute to the development of more effective displacement prediction tools to support the design and execution of safe and sustainable underground construction.

## II. MATERIALS AND METHOD

The study area is located in the center of Ho Chi Minh City, a region characterized by complex and diverse geological conditions. This area features a 7.5 m thick clay layer overlying 32.5 m thick sand layers, with the groundwater table at a depth of -4 m. These soil layers have different mechanical properties, resulting in variations in the load-bearing capacity and the deformation behavior of the ground. Understanding these geological characteristics is crucial for constructing analytical models and accurately predicting the behavior of retaining walls under real-world conditions.

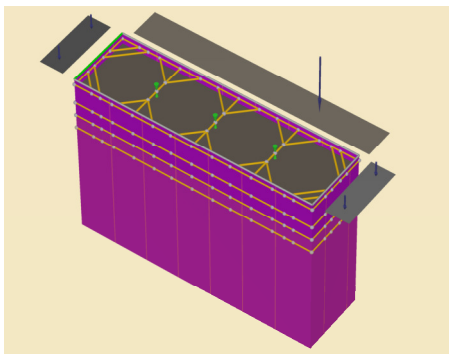


Fig. 1. Excavation simulation

The barrette wall used in this study has a length of 30 m and is designed with four different thicknesses: 400, 600, 800, and 1000 mm. The barrette wall is reinforced with a support system consisting of four layers positioned at depths of -1, -4.6, -7.1, and -9.6 m. The excavation pit measures 11×44 m and has a depth of -15 m, representing typical conditions for underground projects in urban areas, as shown in Figure 1. This support system plays a crucial role in stabilizing the barrette wall and controlling lateral displacement during construction and operation.

The FEM models for the simulations are divided into 10-node triangular elements to increase accuracy [15, 16]. Geotechnical parameters of the soil, such as the modulus of elasticity and the shear strength, are determined through laboratory tests and geotechnical survey reports to ensure model realism. The analysis is carried out under assumptions of the linear elastic properties of the soil and structure. Actual measurements of lateral displacement are performed using an inclinometer at key points on the 800 mm thick barrette wall. This is done to verify the FEM simulation results and improve the reliability of the study. Data are recorded layer by layer, allowing precise comparisons between observed and predicted results. The ANN model is used to predict lateral displacement based on input data from FEM results [17-19]. It is a feedforward network comprising three hidden layers with 64, 32, and 16 neurons, respectively, using ReLU activation functions, and a linear output layer with two neurons corresponding to the  $U_x$  and  $U_y$  displacements. Input variables include position ( $x, y, z$ ), depth, wall thickness, and stress and moment parameters such as  $N_1, N_2, Q_{12}, Q_{13}, Q_{23}, M_{11}, M_{22},$  and  $M_{12}$ . The model was trained over 100 epochs using the Adam optimizer and Mean Squared Error (MSE) as the loss function, ensuring stable convergence and low prediction error. The ANN is trained to identify non-linear relationships between input data and displacement results, ensuring accurate predictions of  $U_x$  and  $U_y$  displacements under complex real-world conditions.

## III. RESULTS

The results include lateral displacements ( $U_x$  and  $U_y$ ), moments (Moment), axial forces (Axial force), and shear forces (Shear force) at different depths and wall thicknesses. Lateral displacements show a decreasing trend as the thickness of the barrette wall increases, as shown in Table I. At an excavation depth of -13.1 m, the lateral displacement  $U_x$  for a 400 mm thick wall is 20.14 mm, higher than the 16.641 mm for the 600 mm thick wall and the 14.643 mm for the 800 mm thick wall. Similarly, the displacement decreases to 13.273 mm when the wall thickness reaches 1000 mm. For  $U_y$  displacement, at the same excavation depth of -13.1 m, the 400 mm thick wall exhibits a lateral displacement of 50.951 mm, while the 600 mm and 800 mm thick walls show displacements of 43.478 mm and 38.937 mm, respectively. The 1000 mm thick wall records the lowest  $U_y$  displacement of 35.588 mm. These results reflect the relationship between wall thickness and structural stability, demonstrating that increasing wall thickness significantly contributes to the reduction of lateral displacement under complex geological conditions.

At an excavation depth of -10.1 m, the 400 mm thick wall has an almost negligible  $U_x$  lateral displacement (0.014 mm), while the  $U_y$  displacement reaches 0.037 mm. For the 800 mm thick wall,  $U_x$  displacement significantly increases to 10.728 mm, and  $U_y$  displacement reaches 29.375 mm, indicating greater displacements at shallower depths when subjected to overhead loads. A larger thickness, specifically 1000 mm, considerably reduces  $U_x$  displacement to 0.01 mm and  $U_y$  displacement to 0.027 mm, demonstrating the better load-bearing capacity of thicker walls under similar conditions.

TABLE I. SUMMARY OF HORIZONTAL DISPLACEMENT RESULTS

Depth (m)	Thickness (mm)	Horizontal displacement (mm)	
		Ux	Uy
-13.1	400	20.14	50.951
-13.1	600	16.641	43.478
-13.1	800	14.643	38.937
-13.1	1000	13.273	35.588
-10.1	400	0.014	0.037
-10.1	600	0.012	0.032
-10.1	800	10.728	29.375
-10.1	1000	0.01	0.027
-7.6	400	9.939	26.925
-7.6	600	8.469	24.243
-7.6	800	7.645	22.241
-7.6	1000	6.973	20.551

The analysis of moments reveals significant differences among the various wall thicknesses. At a depth of -13.1 m, the 400 mm thick wall shows the maximum M11 moment at 380.097 kNm/m and a minimum of -556.895 kNm/m, whereas these values rise to 1308.61 kNm/m and -1242.61 kNm/m for the 1000 mm thick wall. This indicates that thicker walls help reduce moment variation and enhance structural stability. For axial forces at the same depth, the 400 mm thick wall has a maximum N1 value of 2200.938 kN/m and a minimum of -2123.28 kN/m, while the 1000 mm thick wall reaches up to 2853.973 kN/m and -2815.67 kN/m, demonstrating that a greater thickness increases load-bearing capacity and stability. The shear force Q12 shows a similar trend, with the highest values recorded in thicker walls, helping to prevent lateral deformation and improving the structural durability of the barrette wall. These results confirm that increasing wall thickness is an effective measure for enhancing stability and load-bearing capacity under complex conditions.

At the first excavation layer, at a depth of 0 m, the FEM analysis result for Uy displacement is -8.044 mm, while the observed value from the inclinometer is -7.162 mm, indicating a certain discrepancy between the model and the actual data. The correlation coefficient between the FEM and the inclinometer for Uy at this layer is 0.968, as shown in Table II, demonstrating a high level of agreement but with minor errors.

TABLE II. CORRELATION COEFFICIENT RESULTS BETWEEN FEM AND INCLINOMETER FOR UX DIRECTION

Correlation coefficient	Layer 1 (-2 m)		Layer 2 (-5.1 m)		Layer 3 (-7.6)		Layer 4 (-10.1 m)		Layer 5 (-13.1m)	
	FEM	Inclin	FEM	Inclin	FEM	Inclin	FEM	Inclin	FEM	Inclin
Ux	0.973	0.961	0.985	0.985	0.998	0.998	0.999	0.999		
Uy	0.968	0.979	0.981		0.987		0.993			

At the third excavation layer, at a depth of -2 m, the displacement value from FEM is -11.419 mm compared to -12.512 mm from the observational data, with a correlation coefficient of 0.981 for Uy, confirming that FEM accurately replicates the lateral displacement trend at this layer. For the fifth excavation layer at a depth of -5.5 m, FEM predicts a Uy displacement of -19.843 mm, while the inclinometer records -18.389 mm, with a correlation coefficient of 0.993 indicating a very high level of agreement between the two data sources.

At greater depths, such as -10 m at the fourth excavation layer, the Uy displacement from FEM is -27.717 mm compared to -28.538 mm from the Inclinometer. The correlation coefficient here reaches 0.987, demonstrating the high accuracy of the FEM model under deeper conditions. For Ux, the correlation coefficient also shows significant alignment, with a value of 0.998 at this layer, as shown in Figure 2.

At a depth of -15 m in the fifth excavation layer, the FEM displacement is -38.357 mm, while the inclinometer data shows -38.202 mm. At a depth of -30 m, FEM records a Uy displacement of -13.900 mm compared to -14.572 mm from the inclinometer, with a correlation coefficient for Uy reaching 0.993, indicating the model's high reliability, as shown in Figure 3.

This analysis of correlation coefficients confirms that FEM can predict lateral displacements with high accuracy, especially at deeper layers. This underscores the importance of validating the model with real data to enhance the reliability and effectiveness of geotechnical analyses.

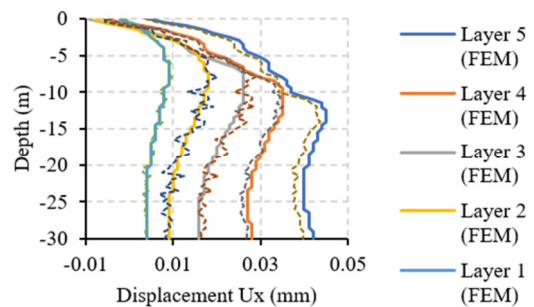


Fig. 2. Lateral displacement results for Ux at the observation point (-2, 5.5).

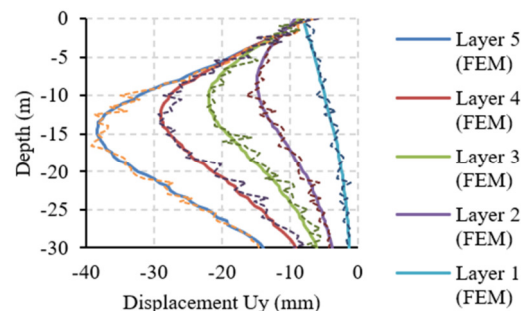


Fig. 3. Lateral displacement results for Uy at the observation point (-2, 5.5).

The ANN model demonstrated high efficiency in predicting lateral displacements of Ux and Uy based on input data from FEM analysis. Performance evaluation metrics for the ANN model included MSE, RMSE (Root Mean Squared Error), MAE (Mean Absolute Error), and the R<sup>2</sup> coefficient, reflecting the model's predictive accuracy and reliability. For Ux displacement, the R<sup>2</sup> coefficient reached a high value of 0.9887, indicating a strong alignment between predicted and actual values and confirming that ANN can accurately predict Ux displacement within the data range used.

Similarly, for Uy displacement, the R<sup>2</sup> coefficient was 0.9998, demonstrating that the ANN model can reliably and precisely replicate Uy displacement. MSE was 0.032891, RMSE reached 0.181357, and MAE was 0.097682. These metrics affirm that ANN can be effectively used as a powerful supplementary tool to FEM for predicting lateral displacements.

The analysis of feature importance on the predicted displacement results showed that the y-coordinate (m) had the highest impact, with an importance score of 115.1896. Depth also played a significant role, with an influence score of 41.27095, followed by the x (m) and z (m) coordinates, with scores of 22.97574 and 14.36987, respectively. Wall thickness was also noted to have a considerable effect, with an importance score of 10.40327. Other factors, such as axial forces (N1, N2), moments (M11, M22, M12), and shear forces (Q12, Q13, Q23), had a lower influence but still contributed to refining the prediction results, as shown in Table III.

TABLE III. FEATURE IMPORTANCE

Feature	Importance	Feature	Importance
y (m)	115.1896	M22 (kN m/m)	0.389615
Depth	41.27095	N1 (kN/m)	0.215018
x (m)	22.97574	Q13 (kN/m)	0.013306
z (m)	14.36987	M12 (kN m/m)	0.007637
Thickness	10.40327	Q12 (kN/m)	0.00544
N2 (kN/m)	0.719199	Q23 (kN/m)	0.005001
M11 (kN m/m)	0.65177		

The chart of feature importance shows that positional factors and depth significantly influence lateral displacement prediction outcomes, emphasizing that geographical and structural factors play a crucial role in the modeling, as shown in Figure 4. The error distribution chart (MAE) over epochs demonstrates the stability of the model during training, with errors gradually decreasing over time, confirming the effectiveness of neural network optimization. The 3D error distribution chart, as shown in Figure 5, further clarifies the extent of errors within the model in a three-dimensional space. This chart shows that the distribution of errors is mainly concentrated at low levels, demonstrating that the ANN model can make predictions with minimal errors for both target variables Ux and Uy. The clustering of data points within a low error range is evidence of the high accuracy of the model.

Figure 6 illustrates the model optimization process of the model over training epochs. The loss chart shows a gradual decrease during training, confirming that the model has converged to a stable state. The MAE is also depicted across each epoch, demonstrating a significant decrease during the initial iterations and reaching stability in later epochs. This result reinforces the conclusion that the ANN model was trained effectively, ensuring both accuracy and consistency in displacement predictions.

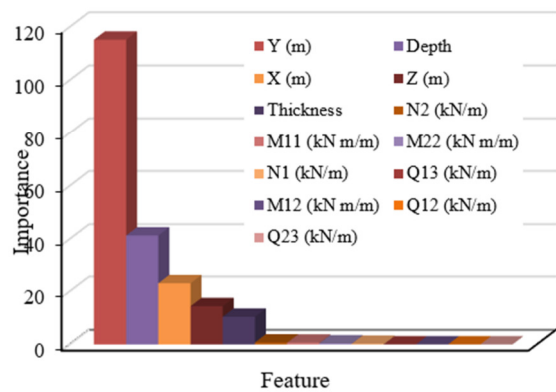


Fig. 4. Feature importance.

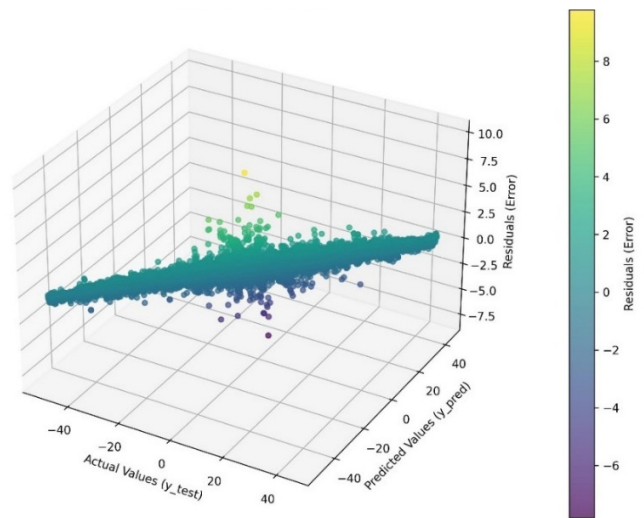


Fig. 5. 3D error distribution.

#### IV. DISCUSSION

The FEM model has been proven effective in simulating the lateral displacement of barrette walls with different thicknesses. The results show that as the wall thickness increases from 400 to 1000 mm, the lateral displacement significantly decreases, reflecting higher structural stability. This aligns with the theory of increased load-bearing capacity in thicker structures. However, the discrepancy between FEM displacement values and observational data from the inclinometer, with correlation coefficients of 0.987 for Uy and 0.985 for Ux, indicates that while the FEM model is highly reliable, it still possesses certain errors.

When applied to predict lateral displacement based on FEM data, the ANN model achieved impressive accuracy, with R<sup>2</sup> values of 0.9887 for Ux and 0.9998 for Uy. This demonstrates the strong ability of the ANN to learn and replicate displacement models from complex data. Variables such as y-coordinate and depth play critical roles in prediction, showing that ANN can complement FEM by providing more precise predictions in scenarios where numerical models may lack detail. ANN not only enhances analysis efficiency but also extends FEM's applicability to other geotechnical problems.

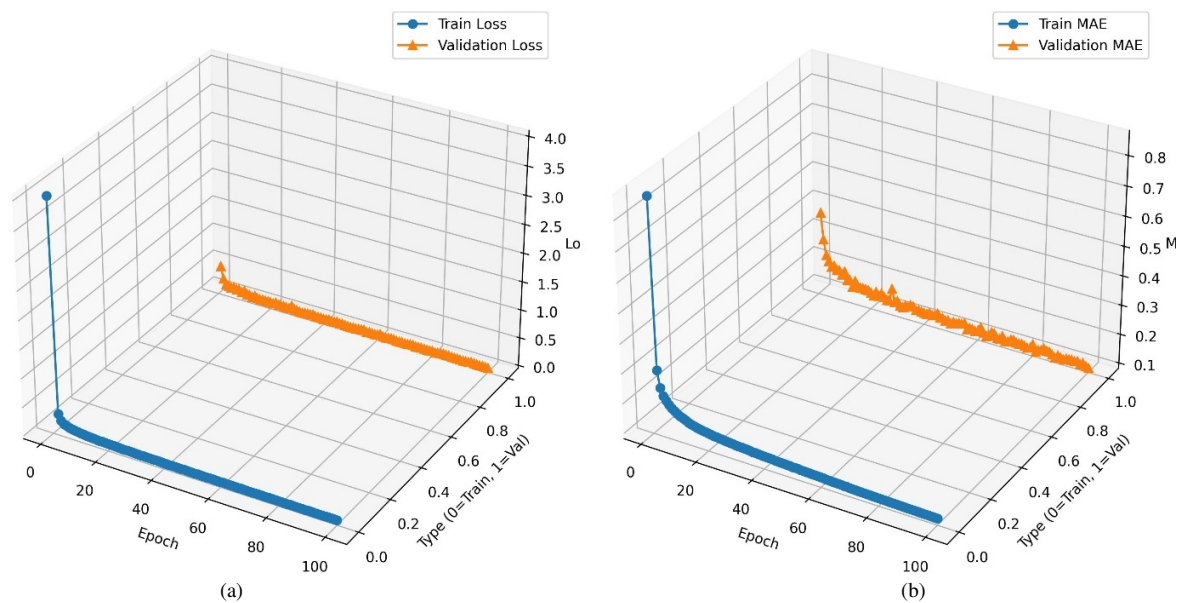


Fig. 6. Loss (a) and MAE (b) graphs.

Compared to previous studies, these findings are consistent with approaches that combine FEM with artificial intelligence to predict deformations under complex geological conditions, such as those caused by earthquakes. Additionally, the integration of machine learning into stress modeling has proven effective in capturing nonlinear material behavior, reinforcing the perspective that artificial neural networks can serve as a powerful tool in analyzing and predicting complex mechanical phenomena. However, this study acknowledges limitations, including the need to improve the ANN model by enhancing the quantity and quality of the input data and considering additional environmental factors, such as heavy rain or seismic activity, which could further improve the prediction accuracy.

## V. CONCLUSIONS

The results of this study show that the FEM model has high accuracy and reliability in predicting the lateral displacement of barrette walls under different geological conditions. FEM analysis demonstrated that increasing the wall thickness from 400 to 1000 mm significantly reduces the lateral displacement, reflecting higher load-bearing capacity and wall stability in complex excavation environments. The high correlation coefficients of 0.987 for  $U_y$  and 0.985 for  $U_x$ , when compared to the inclinometer data, reinforce the reliability of the FEM model in simulating real-world conditions. However, minor discrepancies between the model and actual results suggest that further adjustments may be needed to achieve even higher accuracy. The ANN model, when applied to predict displacement based on FEM data, showed exceptional predictive capacity. High-performance metrics, with  $R^2$  values of 0.9998 for  $U_y$  and 0.9887 for  $U_x$ , confirm that ANN can learn and model complex relationships in displacement data. This indicates that ANN is not only an effective supplementary tool but can also extend FEM's capacity in predicting lateral displacements with higher accuracy, particularly in cases where geological and loading conditions are too complex to be fully captured by FEM alone. The precise predictive ability of ANN

paves the way for developing decision-support tools during the design and construction phases, ensuring that design strategies are optimized based on more accurate structural behavior predictions.

Given these positive outcomes, the application of the FEM and ANN models can be recommended for various geotechnical engineering projects, such as underground infrastructure, retaining walls, and flood embankments in urban areas. Utilizing ANN in combination with FEM in complex analyses can enhance the effectiveness and reliability of predictions, thus improving design, optimizing costs, and enhancing project safety. This is particularly beneficial in the context of increasing demands for safety and structural stability in large cities and areas with complex geological conditions.

## REFERENCES

- [1] A. B. Ekmen and Y. Avci, "Development of novel artificial intelligence functions based on 3D finite element method using February 6 Kahramanmaraş Seismic Records for earthquake effects prediction in various soils," *Engineering Geology*, vol. 336, Jul. 2024, Art. no. 107570, <https://doi.org/10.1016/j.enggeo.2024.107570>.
- [2] P. Fazily and J. W. Yoon, "Machine learning-driven stress integration method for anisotropic plasticity in sheet metal forming," *International Journal of Plasticity*, vol. 166, Jul. 2023, Art. no. 103642, <https://doi.org/10.1016/j.ijplas.2023.103642>.
- [3] M. Fisonga, Y. Hu, S. Han, Y. Deng, and R. B. Kaunda, "Numerical-geostatistical-based approach to investigate the earth pressure evolution within the large grid wall foundation under adjacent surcharge loading," *Computers and Geotechnics*, vol. 167, Mar. 2024, Art. no. 106056, <https://doi.org/10.1016/j.compgeo.2023.106056>.
- [4] P. T. Nguyen, L. Nhat Vo, T. X. Dang, H. V. V. Tran, and T. A. Nguyen, "Assessing Barrette Wall Stability in Critical Sections during Excavation Using Statistical Testing," *Civil Engineering and Architecture*, vol. 12, no. 6, pp. 3797–3809, Nov. 2024, <https://doi.org/10.13189/cea.2024.120606>.
- [5] T. X. Dang, L. N. Vo, P. T. Nguyen, H. V. V. Tran, and T. A. Nguyen, "Integration of FEM-ANN Methods for Predicting the Horizontal Displacement of Barrette Walls," *Engineering, Technology & Applied*

- Science Research, vol. 15, no. 3, pp. 22246–22251, Jun. 2025, <https://doi.org/10.48084/etasr.10026>.
- [6] M. M. El Gendy, H. M. H. Ibrahim, and I. A. El Arabi, "Developing the composed coefficient technique for analyzing laterally loaded barrettes," *Innovative Infrastructure Solutions*, vol. 5, no. 2, Aug. 2020, Art. no. 43, <https://doi.org/10.1007/s41062-020-00294-y>.
- [7] D. Liu, P. Lin, C. Zhao, and J. Qiu, "Mapping horizontal displacement of soil nail walls using machine learning approaches," *Acta Geotechnica*, vol. 16, no. 12, pp. 4027–4044, Dec. 2021, <https://doi.org/10.1007/s11440-021-01345-z>.
- [8] T. Pradeep, A. GuhaRay, A. Bardhan, P. Samui, S. Kumar, and D. J. Armaghani, "Reliability and Prediction of Embedment Depth of Sheet pile Walls Using Hybrid ANN with Optimization Techniques," *Arabian Journal for Science and Engineering*, vol. 47, no. 10, pp. 12853–12871, Oct. 2022, <https://doi.org/10.1007/s13369-022-06607-w>.
- [9] D. Dupuy, N. Odier, C. Lapeyre, and D. Papadogiannis, "Modeling the wall shear stress in large-eddy simulation using graph neural networks," *Data-Centric Engineering*, vol. 4, 2023, Art. no. e7, <https://doi.org/10.1017/dce.2023.2>.
- [10] L. Liang, M. Liu, C. Martin, and W. Sun, "A deep learning approach to estimate stress distribution: a fast and accurate surrogate of finite-element analysis," *Journal of The Royal Society Interface*, vol. 15, no. 138, Jan. 2018, Art. no. 20170844, <https://doi.org/10.1098/rsif.2017.0844>.
- [11] S. M. Zhang, T. K. Yuan, Y. K. Zhou, D. H. Li, and K. H. Zhuo, "The Research Review of Underground Continuous Wall on Deformation Characteristic," *Applied Mechanics and Materials*, vol. 580–583, pp. 224–230, 2014, <https://doi.org/10.4028/www.scientific.net/AMM.580-583.224>.
- [12] T. Xue, S. Adriaenssens, and S. Mao, "Learning the nonlinear dynamics of mechanical metamaterials with graph networks," *International Journal of Mechanical Sciences*, vol. 238, Jan. 2023, Art. no. 107835, <https://doi.org/10.1016/j.ijmecsci.2022.107835>.
- [13] U. S. Khan, M. Ishfaq, S. U. R. Khan, F. Xu, L. Chen, and Y. Lei, "Comparative analysis of twelve transfer learning models for the prediction and crack detection in concrete dams, based on borehole images," *Frontiers of Structural and Civil Engineering*, vol. 18, no. 10, pp. 1507–1523, Oct. 2024, <https://doi.org/10.1007/s11709-024-1090-2>.
- [14] A. Pais, J. L. Alves, and J. Belinha, "Using Artificial Neural Networks to Predict Critical Displacement and Stress Values in the Proximal Femur for Distinct Geometries and Load Cases," in *Cutting Edge Applications of Computational Intelligence Tools and Techniques*, K. Daimi, A. Alsadoon, and L. Coelho, Eds. Springer Nature Switzerland, 2023, pp. 21–32.
- [15] C. M. Wai, A. Rivai, and O. Bapokutty, "Modelling optimization involving different types of elements in finite element analysis," *IOP Conference Series: Materials Science and Engineering*, vol. 50, Dec. 2013, Art. no. 012036, <https://doi.org/10.1088/1757-899X/50/1/012036>.
- [16] H. Kim and D. Sohn, "A new finite element approach for solving three-dimensional problems using trimmed hexahedral elements," *International Journal for Numerical Methods in Engineering*, vol. 102, no. 9, pp. 1527–1553, Jun. 2015, <https://doi.org/10.1002/nme.4850>.
- [17] W. Samek, G. Montavon, S. Lapuschkin, C. J. Anders, and K. R. Muller, "Explaining Deep Neural Networks and Beyond: A Review of Methods and Applications," *Proceedings of the IEEE*, vol. 109, no. 3, pp. 247–278, Mar. 2021, <https://doi.org/10.1109/JPROC.2021.3060483>.
- [18] J. Wang and M. S. Rahman, "A neural network model for liquefaction-induced horizontal ground displacement," *Soil Dynamics and Earthquake Engineering*, vol. 18, no. 8, pp. 555–568, Dec. 1999, [https://doi.org/10.1016/S0267-7261\(99\)00027-5](https://doi.org/10.1016/S0267-7261(99)00027-5).
- [19] H. Nguyen *et al.*, "Optimizing ANN models with PSO for predicting short building seismic response," *Engineering with Computers*, vol. 36, no. 3, pp. 823–837, Jul. 2020, <https://doi.org/10.1007/s00366-019-00733-0>.